ILC Beam-Parameters and New Physics

Mikael Berggren *

DESY
Nothkestrasse 85, Hamburg - Germany

A brief overview of the linear collider design is given, with emphasis on the elements of particular importance for the performance. The modifications of the RDR design suggested in the SB2009 proposal are presented, once again with emphasis on those item that have most impact on the performance. In particular, the effects on New Physics channels are studied, by two examples: the analysis of the properties of $\tilde{\tau}$:s in the SUSY benchmark point SPS1a', and the model-independent Higgs recoil mass analysis. It is shown that for both these cases, the SB2009 design performs significantly worse than the RDR design: For the $\tilde{\tau}$ analysis, the uncertainties on both the mass and cross-section determination increases by 20 % (or 35 % if the travelling focus concept is not deployed). For the Higgs analysis, the corresponding increase in uncertainty is found to be 70 % both for cross-section and mass (or 100 % without travelling focus). For both channels, the deterioration is to a large part due to the move of the positron source to the end of the linac.

1 Introduction

This note is a combination of two talks given at LCWS 2010. One talk was given in the machine-detector interface session, and was mainly aimed in explaining our findings on the physics impact of different options for the design of the ILC to the accelerator community. The other invited talk had the opposite focus: to explain to the physics community what options were discussed for the machine and how and why they influence the physics reach of the ILC. The latter talk was given in the SUSY and New Physics session.

The note is organised as follows: In the first section, a brief description of the different subsystems of the ILC is given, with particular emphasis on which design choices mostly influence the performance, in terms of total luminosity, luminosity on-peak, polarisation, quality of the beams, machine background, and energy reach. The energy dependence of these factors is also discussed. The second section presents the SB2009 proposal, and in the third section the impact of the SB2009 proposal on the performance on two key-channels ($\tilde{\tau}$:s in the SUSY point SPA1a' and the SM Higgs) is discussed. Finally, conclusions are given, and a brief summary is done of the current activities within the GDE to alleviate the performance problems arising from the new base-line design pointed out here and in other contributions to LCWS 2010.

2 The linear collider

In an ideal e^+e^--collider, one would have an exactly known initial e^+e^- state. Both beams would be fully polarised, and the intensity of the beams would be such than one would have as many events as needed not to be statistics-limited at any E_{CMS} for all interesting physics

*Work supported by the DFG through the SFB (grant SFB 676/1-2006) and the Emmy-Noether program (grant LI-1560/1-1)

channels. Furthermore, one would have pure electron/positron beams, with negligible background from the machine or from $\gamma\gamma$ events.

Clearly, none of these properties will be present in any actually buildable accelerator. On the contrary, in a real linear collider, the beam energy has both initial and beam-beam induced spread. The degree of positron polarisation will be rather low ($\sim 30\,\%$), and electron polarisation will be $< 100\,\%$. Obviously, the luminosity will be limited, so that many physics observables will remain statistics limited, even at the end of the life-span of the accelerator. Due to beam-beam effects, the beams will be mixed lepton and photon ones, and there will be huge numbers of low energy background particles from the machine. Clearly, there is no way to avoid background from $\gamma\gamma$ events.

To create the beams, one must have sources of electrons and positrons, and the two need to employ different technologies. The beams should be as well defined as possible, so the initial random spread in energy and direction should be reduced, which is done in the damping system. The main system of the accelerator, which will allow to attain the high centre-of-mass energies required is the main linac. The beams need to be brought into collision at the centre of the detectors, and it is the beam delivery and final focus systems that are employed to achieve this.

In the following sub-sections, some details are given on the implementation of each of these sub-systems at the ILC. The information is taken from the Reference Design Report [1] (the RDR), and Figure 1 shows schematic layouts for the RDR and SB2009 [2] designs.

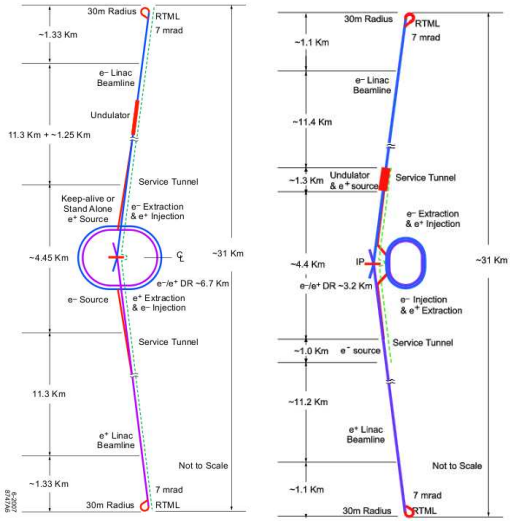

Figure 1: ILC, RDR [1] (left) and SB2009 [2] (right) designs

2.1 Sources

The electron source comprises polarised lasers shining on photo-cathodes, which are specially designed GaAs/GaAsP super-lattice structures yielding electrons with high polarisation, see Figure 2. The emitted electrons are collected and pre-accelerated, and then sent to the damping system. Positrons are obtained by letting a high energy electron beam pass an helical undulator acting as a FEL, to produce photons of high intensity, high polarisation and high energy ($\sim$ 10MeV). These hit a target to produce e^+e^--pairs, see Figure 2. To avoid damage to the target, it is designed as a rotating wheel. The electron beam must have an energy of at least 150 GeV: at lower energies the positron yield becomes so low that the positron bunches are not filled to full capacity, and the over-all luminosity will decrease.

Like the electrons, the positrons are then collected, pre-accelerated and sent to the damping system. The electrons used to produce the photons are the same as those that will be delivered to the detectors. Due to the effect of the helical undulator, the electron beam will therefore obtain an additional energy dispersion.

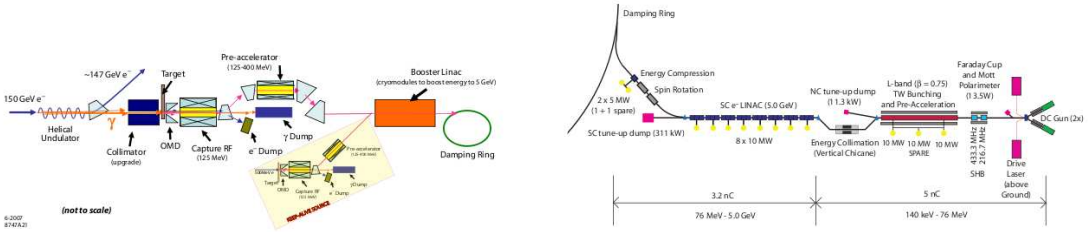

Figure 2: Electron (left) and positron (right) sources. From [1].

2.2 Damping system

When emerging from the sources, the dispersion both in angle and energy of both beams are far to large to be accelerated and delivered to the detectors. This dispersion is reduced by sending the beams (now at $\sim$ 5 GeV) to rings where they pass wigglers which make them cool off by synchrotron radiation. The particle bunches in the damping ring are kicked out, one-by-one, every $\sim$ 100 ns to make a bunch train comprising $\mathcal{O}(1000)$ bunches (2625 in the RDR design). The bunches in the damping-rings are separated by a few ns, given by the ratio of the circumference of the damping ring to the number of bunches. Therefore the kickers must be able to switch on or off in a few ns, which is at the limit of current technology. This procedure (cooling and bunch-train assembly) must be completed in the 200 ms between bunch trains. The damping rings are at the centre of the complex, so it is needed to transport the trains $\sim$ 15 km to the start of the main linac after damping.

2.3 Main linac

The main linac is made of supra-conducting RF cavities each containing 9 accelerating cells. The accelerating gradient is 31.5 MV/m, which is the foreseeable limit of this technology. One RF unit contains three cryo-units, two of which contain 9 cavities, and one which contains 8 cavities and a focusing quadrupole. There are 278 RF units in the positron linac, and 282 in the electron one. There are more in the latter, because the energy lost in the undulator must be compensated for. How many particles one can get at the experiment per time-unit depends on how much power is fed into the cavities, which in turn depends on how many klystrons are installed along the accelerator. How these system are arranged in the RDR two-tunnel design can be seen in Figure 3. In the RDR design, the positron source is placed at the point where the electron beam reaches 150 GeV, about 6 km from the IP, and electrons can be delivered to the experiment at any energy between 50 and 250 GeV, by appropriately accelerating or decelerating them in the remaining part of the main linac.

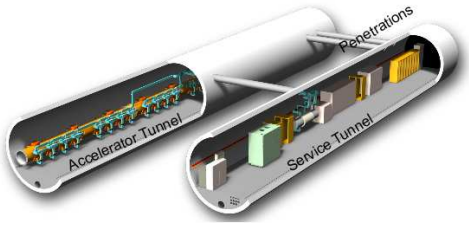

Figure 3: A section of the main linac. From [1].

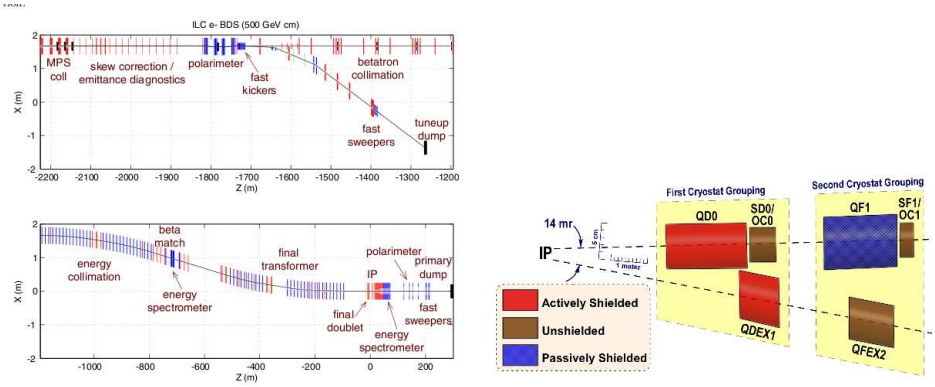

Figure 4: Beam delivery system (left) and Final focus (right). From [1].

2.4 BDS and final focus

The last two km of the accelerator is the Beam Delivery System (the BDS). It's purpose is multiple. It should monitor and measure the beam-properties, and clean the beam from halo particles. It should also protect the detectors, since anything the beam hits at this location will give secondaries - E_{beam} could be up to 500 GeV - that might hit and damage the detectors. A schematic of the BDS is shown to the left in Figure 4.

The final focus system (Figure 4, right) is the last 20 m before the detectors. It focuses the beams to few 100 nm horizontally, and few nm vertically at the centre of the detector. There are several limiting factors on how strongly the beams can be focused, both from fundamental optics, from beam-beam interactions and from stability against ground-motion. In addition, stronger focusing inevitably induces more background in the detectors.

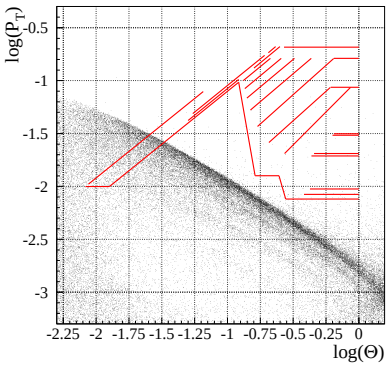

Figure 5: Beam-strahlung particles in ILD.

2.5 Beam-strahlung

Due to the very strongly focused beams, both the electric and magnetic fields induced by one beam have a large bending power on the other one. As a consequence the primary beam is focused by the other beam, and will emit a large amount of synchrotron radiation [3][4]. The emission of synchrotron radiation widens the distribution of the primary $e^{\pm}$ energy. In addition, the synchrotron photons can undergo Compton backscattering, which in turn has several consequences: It yields a photon component of beam, and a long tail to lower energies for the $e^{\pm}$ beam. The resulting relative energy-loss due to beam-strahlung is given by $\delta_{BS} \propto (E_{cm}/\sigma_z) \times (n^2/(\sigma_x + \sigma_y)^2)$, where $\sigma_{x,y,z}$ are the sizes of

the beam in the x,y or z direction, and n is the number of particles in each bunch [3]. Furthermore, the synchrotron photons can interact with photons (synchrotron ones, or virtual ones) in the other beam, yielding $e^{\pm}$-pairs. Necessarily, one of the particles in the pair will have a charge *opposite* to that of its parent beam. These particles gets *de-focused* rather than focused by the other beam, and is the origin of the pair background. Of these wrong-sign $e^{\pm}$:s, the ones at the outer edge of the beam will encounter the largest bending force. The force is independent of the (longitudinal) momentum of the particle, which means that p_T and θ anti-correlates for the pair background, and that it accumulates at a quite sharp edge in the p_T-θ plane. To study the effect of the pair background on the detector, it is useful to also draw the detector in these coordinates: Place each detector element at the p_T-θ corresponding to the p_T and θ a particle should have to turn back at the radius and z of the element. As an example, Figure 5 shows the distribution of the beam-strahlung pairs in ILD in these coordinates, for RDR design with nominal beam-parameters. The pairs were generated with GuineaPig [4], and the simulation shows that there are some 124000 particles created per bunch-crossing.

2.6 Luminosity

The Luminosity(L) is defined as the density of particles that pass each other per time-unit, ie. $L = N^2/(t \times A)$, where A is the transverse area of the beam at the interaction point. The number of interactions per time unit is therefore L multiplied by the cross-section for the considered physics process. For the number of particles passing each other (N) per time-unit, one has that $N^2/t = n^2 N_{bunch} f_{rep}$, where n is the number of particles in the bunch, N_{bunch} is the number of bunches in the train, and f_{rep} is the number of trains per second. One can note that RF-power (P_{RF}) needed also depends on n, N_{bunch}, and f_{rep} : $P_{RF} = E_{cm}(nN_{bunch}f_{rep}) \times \eta$, where η is the efficiency of the transfer from the RF-system to the beam. Hence, $L \propto P_{RF} n/AE_{cm}$. Furthermore, for A, the cross-section of beams at the IP, one has that $A \propto \sigma_x \times \sigma_y$, where σ_x and σ_y are the horizontal and vertical sizes of the beam, respectively. These sizes are given by the final focus system, the damping system and the γ factor of the beams (proportional to the beam energy): $\sigma \propto \sqrt{\epsilon\beta} = \sqrt{\epsilon_{norm}\beta/\gamma}$. Here ϵ is the emittance, ϵ_{norm} is the normalised emittance - which is the figure of merit of the damping system - and β, the focusing-power of the final focus system. It therefore follows that to get high L, $\sigma_x \times \sigma_y$ should be small. However, as mentioned above, the relative energy-loss due to beam-strahlung is inversely proportional to $\sigma_x + \sigma_y$, so to reduce it, this sum should be large. The way to achieve small $\sigma_x \times \sigma_y$ and large $\sigma_x + \sigma_y$ at the same time is to make the σ_x and σ_y as different as possible, ie. to have a flat beam. If $\sigma_y << \sigma_x$, one has $\delta_{BS} \propto (E_{cm}/\sigma_z) \times (n^2/\sigma_x^2)$ and by re-ordering of terms that: $n/\sigma_x \propto \sqrt{\delta_{BS}\sigma_z/E_{cm}}$. Therefore one can write a number of scaling-laws for the luminosity, that puts emphasis on different design-parameters:

1. $L \propto P_{RF} \times \sqrt{\delta_{BS}\sigma_z}/(\sigma_y E_{cm}^{3/2})$, which emphasises the dependence on available RF power.
2. $L \propto (nN_{bunch}f_{rep}) \times \sqrt{\delta_{BS}\sigma_z}/(\sigma_y E_{cm}^{1/2})$, which emphasises the dependence on beam-structure.
3. $L \propto (n^2 N_{bunch} f_{rep})/(\sigma_x\sigma_y) \propto (n^2 N_{bunch} f_{rep} E_{cm})/(\epsilon_{norm}\beta)$, which emphasises the dependence on beam energy and emittance. Note that the price for luminosity in δ_{BS} is hidden in this formulation.

3 RDR and SB2009

The aim of SB2009 proposal [2] is to save cost, while still full-filling the ILC scope document [5].

The main changes wrt. the RDR design is to house the main linac and it's support systems in a single tunnel (meaning a re-design of the RF-system), half the beam power (meaning half as many bunches in the train, which apart from reducing the need for klystrons and cooling by two, would allow to make the damping rings smaller), while keeping the same total luminosity by stronger final focusing, and to move the positron source to end of the linac (easier logistics and higher positron yield).

For the performance of the machine, this design has a number of issues: The decrease of the beam-size will increase δ_{BS}, meaning that the luminosity within 1 % of nominal reduced from 0.83 to 0.72 at 500 GeV. It also gives more overlaid tracks in the detector, and twice as much energy in the low angle calorimeter (the BeamCal). The halving of the number of bunches at constant total luminosity will double the luminosity per bunch-crossing, and hence the probability to have a $\gamma\gamma$ event in the same bunch-crossing as a physics event. The move of the positron source will give lower luminosity below 300 GeV, since - as described above - once the electron beam is below 150 GeV, the positron bunches will not be full. Since the source is at the end of the linac, the option to decelerate the beam after the undulator no longer exists. At 250 GeV, the luminosity would only be third of the RDR value. In addition, at 500 GeV, the electron beam energy-spread will increase from 0.16 % to 0.21 % and the positron polarisation will decrease from 33 % to 22%, as can be seen in Figures 6 and 7.

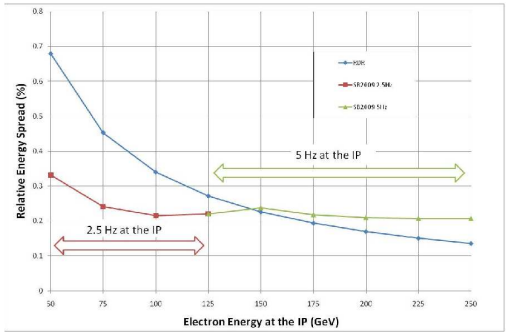

Figure 6: Energy-spread of incoming electron beam. Blue: RDR, Green: SB2009 with 5 Hz rep-rate, Red: SB2009 with 2.5 Hz rep-rate. From [2].

It should be noted that the total luminosity would be unchanged wrt. RDR only if a novel focusing scheme - the Travelling Focus (TF) scheme [6]- can be made practical. If not, the SB2009 proposal would yield a total luminosity 25 % lower than the RDR design already at 500 GeV.

As mentioned above, the increase of δ_{BS} increases the number of beam-strahlung pairs per bunch-crossing by approximately a factor two. The detector-elements for which this is most likely to pose a problem is the vertex-detector, and the BeamCal. In ILD, the vertex detector integrates over a fixed time-window, which is much longer than the

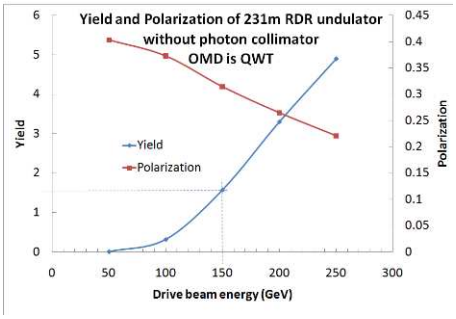

Figure 7: Positron yield and polarisation. From [2].

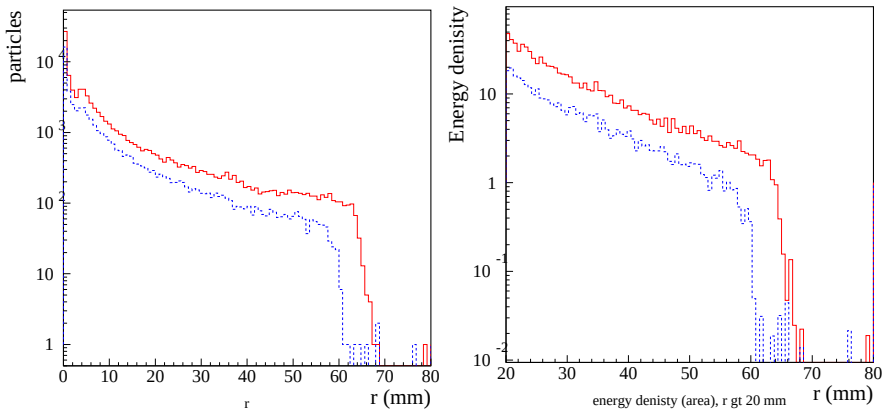

Figure 8: Hits (left) and energy-density (right) in the ILD BeamCal. Solid red: SB2009, Dashed blue: RDR.

intra-bunch separation, so given the fact that the number of bunches per train is reduced by a factor two in the SB2009 design, the number of hits in each time window will be approximately the same for the two designs [7]. The BeamCal, on the other hand, has a read-out fast enough to read single bunch-crossings. As can be seen in Figure 8, showing hit and energy densities for the two designs, the SB2009 would give a doubling of the background levels. The plots show only the GuineaPig simulation, not the full detector simulation, but does include effects of the crossing-angle and compensating magnetic field (the anti-DID field). The issue is whether one still can detect a $\approx$ 250 GeV electron from a $\gamma\gamma$ process over the increased pair-background.

4 SB2009 and physics

Two examples will be used to show the impact on the performance of the different designs: The analysis of the $\tilde{\tau}$ in the SUSY benchmark point SPS1a' [8], which is sensitive to background and polarisation, and the measurement of the mass of a light SM Higgs with the recoil mass method [9], which is sensitive to the luminosity at lower E_{CMS}.

These two examples are not chosen at random. They both represent corner-stone physics cases for the ILC in their own right. This is even more so in view of the LHC program up to 2012: On one hand, the (probable) non-observation of the Higgs in first LHC run would further strengthen the hypothesis that the Higgs is indeed SM-like and has a mass close to the LEP exclusion limit. On the other hand, the current best fit of SUSY as an explanation to all lower energy and cosmological observations, both those that show no tension between the SM and the observations, and those that do (eg. the muon g-2 or the cosmological evidence for the existence of dark matter) is quite close to SPS1a' [13]. If this type of model turns out to be realised in nature, the SUSY spectrum, including the squarks and the gluino, would be light enough that there is a good chance that LHC will discover SUSY in the first run [14]. Hence, and due to the time it would require to modify accelerator designs and to carry out a complete physics analysis, it is prudent that the ILC community already now is prepared to demonstrate that the ILC is right machine for the future, would any of these

observations be done by the time of the 2012 summer conferences.

4.1 SB2009 and physics: $\tilde{\tau}$ in SPS1a'

The ILD analysis of the $\tilde{\tau}$ in SPS1a' is described in detail elsewhere [10][11][12], and only a few remarks are added here.

SPS1a' is a a pure mSUGRA model that predicts SUSY particles just outside what is excluded by LEP and low-energy observations. It is compatible with the observations of WMAP, with the lightest SUSY particle as the Dark Matter candidate. The LSP is the lightest neutralino, $\tilde{\chi}_1^0$. At $E_{CMS} = 500$ GeV, all sleptons are observable, but none of the squarks. The lighter bosinos, up to $\tilde{\chi}_3^0$ (in $e^+e^- \rightarrow \tilde{\chi}_1^0\tilde{\chi}_3^0$) would also be observable. There are a total of 13 distinct channels that would be observable below E_{CMS}=500 GeV, a fact that demonstrates the great advantage of a machine that can deliver high luminosities at a large range of centre-of-mass energies.

In SPS1a', the $\tilde{\tau}_1$ is the Next to Lightest SUSY Particle, the NLSP, and has a mass only 10 GeV above the LSP mass ($M_{\tilde{\tau}_1} = 107.9$ GeV, $M_{\tilde{\tau}_2} = 194.9$ GeV, $M_{\tilde{\chi}_1^0} = 97.7$ GeV/c^2). The fact that the $\tilde{\tau}$ is the NLSP will imply that τ:s are expected in most SUSY decays, so that SUSY will a main background to SUSY. Finally, it can be noted that for 100 % right positron polarisation, and 100 % left electron polarisation ($\mathcal{P}_{beam} = (1, -1)$), the cross-sections for $\tilde{\chi}_2^0\tilde{\chi}_2^0$ and $\tilde{\chi}_1^+\tilde{\chi}_1^-$ production is several hundred fb and BR(X$\rightarrow \tilde{\tau}) > 50$ %, while for $\mathcal{P}_{beam} = (-1, 1)$, these cross-sections almost vanish. Therefore, the degree of polarisation of both beams is a very powerful tool to ameliorate the signal to background ratio.

The mass of the $\tilde{\tau}$ can be obtained either from the decay kinematics or the cross-section. From the kinematics of two body decays it follows that $E_{\tau,\,{}^{min}_{(max)}} \approx \frac{\sqrt{s}}{4}(1-(\frac{M_{\tilde{\chi}_1^0}}{M_{\tilde{\tau}}})^2)(1 \,{}^{-}_{(+)}\, \sqrt{1-\frac{4M_{\tilde{\tau}}{}^2}{s}})$ (neglecting the τ mass). For $\tilde{\tau}_1$ decays the resulting spectrum of the τ:s has $E_{\tau,min} = 2.6$ GeV, $E_{\tau,max} = 42.5$ GeV, hence much of the signal will be hidden in the $\gamma\gamma$ background. For $\tilde{\tau}_2$ one finds that $E_{\tau,min} = 35.0$ GeV, $E_{\tau,max} = 152.2$ GeV. For such a spectrum, the background from $WW \rightarrow l\nu l\nu$ will be an issue, while the $\gamma\gamma$ background is expected to be small. To determine the $\tilde{\tau}$ mass from the spectrum, one needs to accurately measure the end-point of the spectrum of the τ decay products, which is equal to $E_{\tau,max}$. In principle, the τ decay spectrum has a kink at $E_{\tau,min}$, but - at least for $\tilde{\tau}_1$ - this region is completely hidden in the $\gamma\gamma$ background. Therefore, $M_{\tilde{\chi}_1^0}$ must be found from other channels, to be able to determine the $\tilde{\tau}$ mass from the measurement of the end-point. The $\tilde{\tau}$ production cross-section is given by $\sigma_{\tilde{\tau}} = A(\theta_{\tilde{\tau}}, \mathcal{P}_{beam}) \times \beta^3/s$, so that a measurement of this cross-section can be used to determine the mass by $M_{\tilde{\tau}} = E_{beam}\sqrt{1-(\sigma s/A)^{2/3}}$, which does not depend on $M_{\tilde{\chi}_1^0}$.

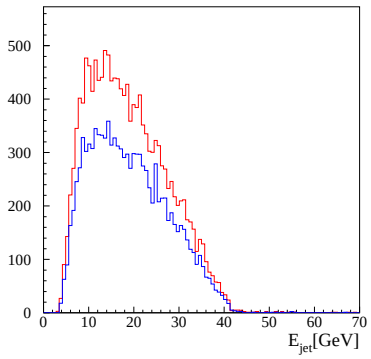

Figure 9: Spectrum of found τ-jets. Blue: Durham, Red: DELPHI

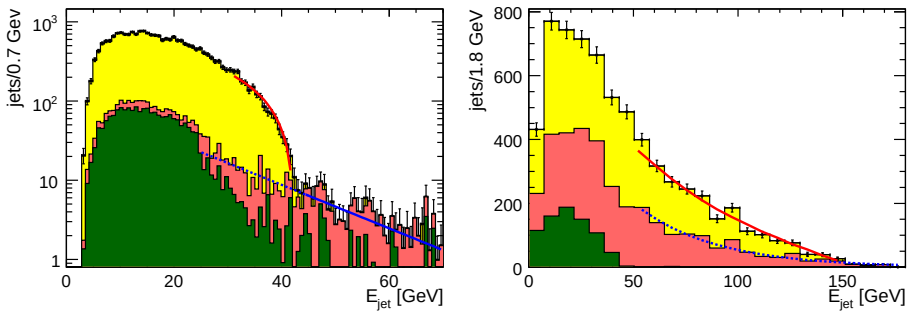

Figure 10: End-point fit for $\tilde{\tau}_1$(left) and $\tilde{\tau}_2$(right). Light grey (yellow) histogram: signal, grey (red) : SM background, dark grey (green): SUSY background. The fit to the background in blue. Fit to total sample: Solid (red) line.

For the ILD LOI [10], all SM processes were fully simulated, as was the full SPS1a' model. The beam-background was estimated by generating 1000 bunch-crossings with GuineaPig, simulating the detector response, and reconstructing these with the full ILD reconstruction procedure, to create a pool of bunch-crossings. For each physics event, one bunch-crossing from the pool was randomly chosen and overlaid before the event was analysed.

The properties of $\tilde{\tau}$ events are:

- Only two τ:s in the final state.
- Large missing energy and momentum.
- High acollinearity, with little correlation to the energy of the τ decay-products.
- Central production.
- No forward-backward asymmetry.

A set of cuts were found to select such events, and to suppress the $\gamma\gamma$ background further cuts were applied, among which was the requirement that there should be no significant activity in the BeamCal, see [11] for details. It should be noted that to get an acceptably low background, it is paramount to have good τ:s only, ie. to have no extra or missing charged tracks. In particular in the presence of beam-background, general jet-finders perform poorly when used to find τ:s. Therefore the DELPHI τ-finder [15] was adopted. It was found to perform better than the Durham algorithm forced to two jets (the ILD default) already without background, see Figure 9.

As has been emphasised above, only the upper end-point is relevant for the determination of the mass from the spectrum. The remaining background in this region needs to be subtracted from the observed distribution, and due to the difference in the amount of poorly known SUSY background, this is done differently for $\tilde{\tau}_1$ and $\tilde{\tau}_2$. In the case of $\tilde{\tau}_1$, a substantial amount of SUSY background remain near the end-point, which can be estimated from the data, by the observation that the region above 45 GeV is signal-free. An exponential distribution was fitted to the data in this region, and was extrapolated to lower jet energies. For $\tilde{\tau}_2$, on the contrary, there is hardly any SUSY processes other than the signal that gives jets above 45 GeV, so the background can be estimated from SM-only simulation. In both cases, the upper tail of the signal spectrum was the obtained by fitting a line to the observed spectrum after subtracting the fitted background. The spectra with signal and background fits are shown in Figure 10.

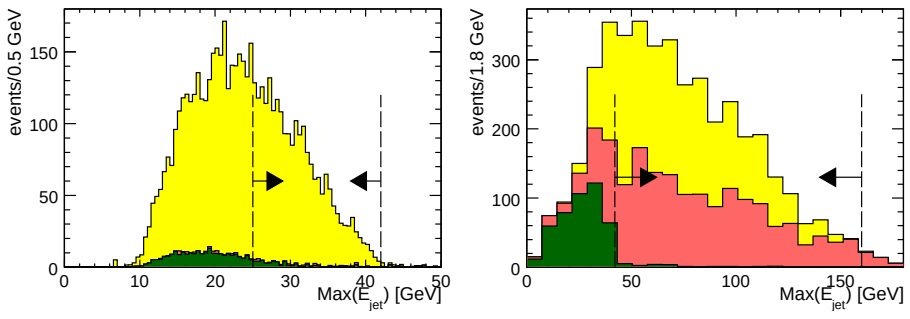

Figure 11: Events selected for the cross-section measurement for $\tilde{\tau}_1$(left) and $\tilde{\tau}_2$(right). The selected events are those with jet-energies in the indicated windows. Legend as in Figure 10.

The poorly known SUSY background is the most important contribution to uncertainty of the cross-section measurement, so efforts need to be made to select region where is is as low as possible. The finally selected events are shown in Figure 11.

The potential effects of the modified machine properties for the $\tilde{\tau}$ analysis include:

- The luminosity decrease for SB2009 without TF.
- The decrease of $\mathcal{P}(e^+)$, which yields more SUSY background, and less signal for $\tilde{\tau}_1$.
- The higher energy-spread of the incoming electron beam will blur the end-point.
- The lower luminosity within 1 % of nominal energy gives a lower signal close to the end-point, where it has it's strongest significance.
- The doubling the amount of beam-strahlung implies more overlaid tracks (real or fake), which destroys the τ topology, and twice as much energy in BeamCal, which increases the $\gamma\gamma$ background.
- The higher luminosity in each bunch-crossing increases the probability for a $\gamma\gamma$ event in the same bunch-crossing as the physics event.

The procedure to modify the fully simulated RDR sample to represent the SB2009 design

	Events for end-point analysis					
case	$\tilde{\tau}_1$			$\tilde{\tau}_2$		
	SM	SUSY	signal	SM	SUSY	signal
RDR	317	998	10466	1518	241	1983
SB09(TF)	814	956	8410	1346	223	1555
SB09(noTF)	611	717	6308	1009	167	1166
	Events for cross-section analysis					
	$\tilde{\tau}_1$			$\tilde{\tau}_2$		
	SM	SUSY	signal	SM	SUSY	signal
RDR	17.6	47.7	2377	1362	33.7	1775
SB09(TF)	17.6	45.7	1784	1194	32.4	1366
SB09(noTF)	13.2	34.3	1337	895	24.3	1025

Table 1: Events after cuts in the $\tilde{\tau}$ analysis for different designs (RDR, SB2009 with of without travelling focus).

		end-point (GeV)		cross-section (%)	
case	#	$\tilde{\tau}_1$	$\tilde{\tau}_2$	$\tilde{\tau}_1$	$\tilde{\tau}_2$
RDR	1	0.129	1.83	2.90	4.24
+SB bck	2	0.144	2.02	3.03	4.72
+SB ppol	3	0.153	2.06	3.31	4.77
+SB spect	4	0.152	2.10	3.52	5.09
+SB noTF	5	0.179	2.42	3.79	5.71

Table 2: Errors on end-point and cross-section for the $\tilde{\tau}$ analysis, with different beam conditions: 1) RDR, 2) RDR, but with background as with SB2009, 3) as 2) but with SB2009:s reduced positron polarisation, 4) Nominal SB2009, with TF, ie. as 3) but with SB2009's beam-spectrum, 5) SB2009 without TF.

was as follows: Our studies of the BeamCal indicates that the energy density in either SB2009 design (with or without TF) is about twice the RDR value at all radii. For the LOI studies, the energy density from the beam-strahlung pairs (ρ_E) was mapped out over the surface of the BeamCal, using the simulation with the RDR beam-parameters. The probability $p(E_e, \rho_E)$ to detect an electron of energy E_e in the BeamCal over a local energy density ρ_E was then determined and parametrised. Hence, the procedure factorises between ρ_E, which depends on the beam-parameters, and $p(E_e, \rho_E)$, which doesn't. Therefore, the SB2009 sensitivity for high-energy beam-remnants could be estimated simply by scaling up ρ_E from it's RDR value by a factor determined to be 2.33, and using the previously determined probability $p(E_e, \rho_E)$. To estimate how many tracks the beam-background would create in the tracking system, a pool of fully simulated bunch-crossings with SB2009 parameters was created and the same procedure as for the LOI-RDR study (see above) was applied. The different beam-spectrum was treated by using the spectra obtained from GuineaPig for both RDR and SB2009 to calculate event-by-event weights based on the beam-energies of each individual event. Finally, it was straight-forward to account for the reduced positron polarisation by correctly adjusting the relative weights of samples generated with either $\mathcal{P}$=(-1,1) or $\mathcal{P}$=(1,-1).

Table 1 shows the number of events after cuts, for the end-point and cross-section analyses, while Table 2 shows the error on the end-point and cross-section, for different machine properties. In Figure 12, these numbers are plotted both as the ratio of uncertainties with respect to the RDR value, and as the increase in data-taking time needed to compensate for the weaker performance.

4.2 SB2009 and physics: SM Higgs at 120 GeV

The potential effect on the measurement of the mass of a light (120 GeV) SM Higgs due to SB2009 modifications of the ILC is the factor 3 to 4 decrease of luminosity at optimal $E_{CMS}(\approx 250$ GeV). This reduced luminosity is, as has been explained above, due to move of positron source. Other aspects of SB2009 should pose no problems: At $E_{CMS} = 250$ GeV, the undulator works at the same working-point for RDR and SB2009, so no differences in incoming beam-spread nor positron polarisation are expected. The Higgs recoil-mass analysis, described in detail in [10] and [16], only depends on the precise measurement of the decay of the Z to high momentum muon or electron pairs. Hence, it is not sensitive to $\gamma\gamma$ background, nor to overlaid background tracks.

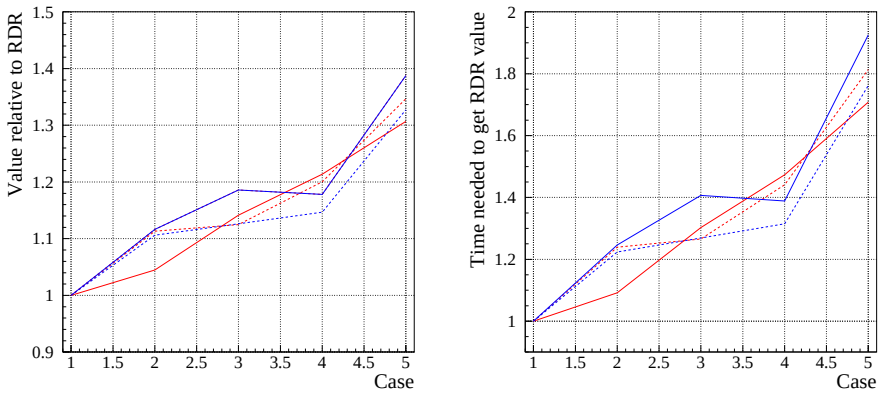

Figure 12: The effect of beam-parameters for the results of the $\tilde{\tau}$ analysis. The left plot shows the uncertainty wrt. the RDR value, while the right one shows the increase in data-taking time needed to achieve the RDR value. Red: cross-section, Blue: end-point, Solid : $\tilde{\tau}_1$, Dashed: $\tilde{\tau}_2$. The numbers on the x-axis are explained in caption of Table 2.

It has been suggested to do the analysis at 350 GeV, where luminosity loss is much less important(20-40 %). However, the cross-section is sizably lower at this energy, and since the lepton-pairs will have higher momenta, the experimental resolution will be worse. Since this channel was not studied at 350 GeV for the LOI, a fast simulation was set up to bring the experience gained from full simulation at 250 GeV to an estimate of the performance at 350 GeV, both for the RDR and SB2009 designs [17]. The fast simulation has been verified with respect to the full simulation at 250 GeV, with RDR parameters, and excellent agreement was found.

One could then compare the recoil-mass peak obtainable with the same running-time at 250 or 350 GeV, for RDR and SB2009. Two observations can be done in Figure 13: As expected, there is a much larger loss of events going from 350 to 250 GeV in the SB2009

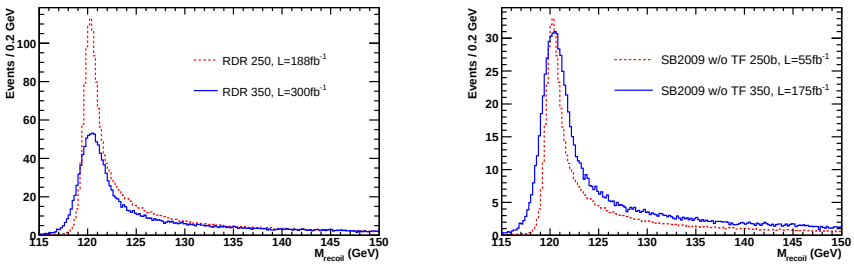

Figure 13: Recoil Mass for the RDR design (left) and the SB2009, without TF (right) for E_{CMS}=250 and 350 GeV

Beam Par	$\mathcal{L}_{\rm int}$ (fb^{-1})	ϵ	S/B	$\Delta(M_H)$ (GeV)	$\delta\sigma/\sigma$
RDR 250	188	55%	62%	0.043	3.9%
RDR 350	300	51%	92%	0.084	4.0%
SB2 TF 250b	68	55%	62%	0.071	6.4%
SB TF 350	250	51%	92%	0.092	4.3%
SB2 noTF 250b	55	55%	62%	0.079	7.2%
SB Wolf 350	175	51%	92%	0.110	5.2%

Table 3: Performance of the Higgs recoil mass analysis for different beam conditions.

design, than what is observed for the RDR design. Furthermore, for both designs, the peak is broader at 350 GeV, which, as can be seen in Figure 14, is due to the deterioration of the momentum resolution at higher track moments. Table 3 shows the details of the deterioration of the measurement wrt. the LOI design.

One can note that for the RDR design, the 250 GeV result is best both for cross-section and mass measurements, while for the SB2009 (TF), the 250 GeV result is best for the mass measurement, while the 350 GeV is the best for the cross-section measurement. Hence, for SB2009, one must choose which running scheme to use: either the mass-measurement will worse by 110 %, but the cross-section only by 10 % with respect to the RDR design, or the mass-measurement will be worse by a more modest 70 %, at the expense that the cross-section will be worse by 65 %.

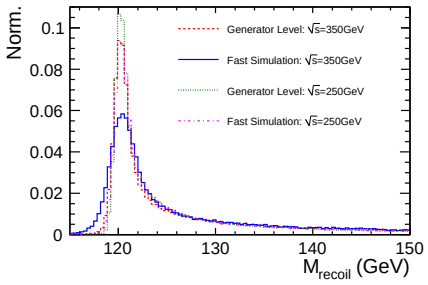

Figure 14: Generated and simulated Recoil Mass for the RDR design, at E_{CMS}=250 and 350 GeV

5 Conclusions and outlook

In section 1, the ILC was briefly described,
and it was pointed out that depending on what is built in to the machine design (P_{RF}, f_{rep}, N_{bunch}, δ_{BS} ...), luminosity scales differently with E_{cm}, and that different machine setups give different luminosity scaling, different polarisation scaling, different energy within 1 % to nominal, and different spread in E_{beam}. The key issues for performance were pointed out, and how they relate to technological challenges for the accelerator design.

From studying the effect of the transition from the RDR to the SB2008 designs on the $\tilde{\tau}$ analysis it was seen that for such "fragile" signals, beam-background influences signal directly. It was also seen that for any "low $\Delta(m)$" ($<$ 10 GeV) signal, beam-background should be taken into consideration when estimating $\gamma\gamma$ background. It was found that effect of replacing the RDR beam-parameters by the SB2009 ones, the measurement quality degrades by 15-20 %, both for the end-point and cross-section measurements, and both for the $\tilde{\tau}_1$ and $\tilde{\tau}_2$ channels. Of this degradation, half comes from the modifications of the positron source, namely the larger spread in E_{CMS}, and the reduction in $\mathcal{P}(e^+)$. It was also shown that the degradation increases to 20-40 %, if the travelling focus concept would

turn out to be unfeasible. It was pointed out that degradation can be compensated for by increasing the data-taking period by 40 % (or 80 % in the no travelling focus case). It was also pointed out that for a low-mass SUSY scenario like SPS1a', many thresholds are expected below E_{CMS}=500 GeV, emphasising the importance of having an accelerator tunable in energy.

By studying the effects of the transition on the SM Higgs recoil-mass analysis, it was observed that the results will not scale with cross-section if the analysis is done a different E_{CMS}, since the detector resolution depends on energy. At E_{CMS} = 250 GeV, the influence on the error on the Higgs mass from the detector resolution is quite small compared to the spread of the beam energy, but already at E_{CMS} = 350 GeV, detector effects dominate the error. It was found that replacing the RDR design by the SB2009 one degrades the quality of the mass measurement by 110%, and the cross-section measurement by 10 % (if the analysis is done at 350 GeV), or by 70 % and 65 % (if it is done at 250 GeV). Without travelling focus, the numbers are 160 % and 30 % (at 350 GeV) or 80 % and 85 % (at 250 GeV). To compensate for these losses in precision by longer data-taking is difficult: at least three times more time need to be spent at an energy where the Higgs channel is likely to be the only channel to study. The loss in performance is in this case completely driven by loss of luminosity at 250 GeV, which is entirely due to move of positron source.

Hence, both these studies arrive at the conclusion that the move of the positron source has a disproportionally large effect on the performance, while the increased background has less of an impact.

Since the presentation of the SB2009 proposal in December 2009, it has been reviewed by the AAP [18] and the PAC [19], and a committee (the "Brau committee") has been set up to review the performance issues the proposal gave rise to. In particular, the effect of the move of the positron source has received much attention. The GDE has subsequently set up a series of work-shops aiming to solve this and other issues by mid-2011, and defined a formal "change control process" for the baseline design of the ILC.

There are no significant financial savings from placing the positron source at the end of the linac. However, from the operational point of view, it is strongly preferred to have it at that location, since this would keep the main linac tunnel free of a potentially delicate sub-system, and rather concentrate it with all other sub-systems (the electron source, the damping rings, BDS, etc.) to a central campus, where access and maintenance would be eased. Several promising schemes are investigated to avoid the large loss of luminosity below E_{CMS} =300 GeV, while still placing the source at the end of the linac. The most probable solution is to use the fact that at lower beam-energies, there is enough spare RF-power to increase the repetition rate to 10 Hz. One would then accelerate every other electron bunch-train to 150 GeV to produce positrons, and every other, at a lower energy, would be sent to the detector. The feasibility of this scheme is under study, in particular with respect to which modifications would be needed to the damping system to accommodate a higher repetition rate.

References

[1] ILC GDE and WWS, Editors N. Phinney, N. Toge, and N. Walker, "International Linear Collider Reference Design Report - Vol. 3: Accelerator", (2007). http://ilcdoc.linearcollider.org/getfile.py?docid=182&name=ILC_RDR_Volume_3-Accelerator&format=pdf

[2] ILC GDE, Editors M. Ross, N. Walker, and A. Yamamoto, "SB2009 Proposal Document", (2009). http://lcdev.kek.jp/SB2009/SB20091217B.pdf

[3] K. Yokoya and P. Chen, "Frontiers of Particle Beams: Intensity Limitations", edited by M. Month and S. Turner, Lecture Notes in Physics Vol. 400 (Springer-Verlag, Berlin), (1990) 415.

[4] D. Schulte, *PhD Thesis*, DESY/Universität Hamburg, **DESY-TESLA-97-08**, (1997).

[5] R. Heuer (chair) "ICFA - Parameters of the linear collider", (2003) http://www.fnal.gov/directorate/icfa/LC_parameters.pdf, and Update, (2006) http://www.fnal.gov/directorate/icfa/para-Nov20-final.pdf.

[6] V.E. Balakin, "Travelling Focus Regime for Linear Collider VLEPP", Proc. 77th ICFA Workshop on Beam Dynamics, Los Angeles, (1991).

[7] K. Wichmann, *These proceedings*, arXiv:1007.2440 (2010),http://arxiv.org/ps/1007.2440.

[8] J. A. Aguilar-Saavedra & al., Eur. Phys. J. **C46** (2006) 43.

[9] P. Garcia-Abia and W. Lohmann, EPJdirect **C2** (2000) 1.

[10] H. Stoeck & al.,(The ILD concept group), "The International Large Detector: Letter of Intent", arXiv:1006:3396 (2010),http://arxiv.org/pdf/1006.3396.

[11] P. Bechtle & al., arXiv:0908:0876 (2009),http://arxiv.org/ps/0908.0876.

[12] P. Schade, *PhD Thesis* DESY/Universität Hamburg **thesis-2009-040**, (2009).

[13] O. Buchmüller & al. Eur. Phys. J **C64** (2009) 391.

[14] H. Baer, V. Barger, A. Lessa, and X. Tata, arXiv:1004.3594v2, (2010), http://arxiv.org/ps/1004.3594v2.

[15] J. Abdallah & al. (DELPHI collaboration), Eur. Phys. J. **C31** (2004).

[16] H. Li, *PhD Thesis*, Université de Paris-Sud, **LAL 09-118**, (2009).

[17] H. Li, "SB2009 Higgs mass and cross section measurement study", *These proceedings*, (2010).

[18] Accelerator Advisory Panel, "Report on the AAP Review in Oxford",**ILC-REPORT-2010-023**, (2010), http://ilcdoc.linearcollider.org/record/26987/files/Report-on-AAP-Review_Jan2010.pdf?version=1

[19] The ILC project advisory committee, "Report of the fourth meeting of the PAC",**ILC-REPORT-2010-025**, (2010), http://ilcdoc.linearcollider.org/record/28235/files/PAC_May-2010-report-final.pdf?version=1.